

***In vivo* determination of the optical properties of muscle with time-resolved reflectance using a layered model**

Alwin Kienle[†] and Thomas Glanzmann[‡]

[†] Department of Biophysics, University of Ulm, Albert-Einstein-Allee 11, D-89081 Ulm, Germany

[‡] Institute of Environmental Engineering, Swiss Federal Institute of Technology (EPFL), CH-1015 Lausanne, Switzerland

Received 26 May 1999, in final form 8 July 1999

Abstract. We have investigated the possibility of determining the optical coefficients of muscle in the extremities with *in vivo* time-resolved reflectance measurements using a layered model. A solution of the diffusion equation for two layers was fitted to three-layered Monte Carlo calculations simulating the skin, the subcutaneous fat and the muscle. Relative time-resolved reflectance data at two distances were used to derive the optical coefficients of the layers. We found for skin and subcutaneous fat layer thicknesses (l_2) of up to 10 mm that the estimated absorption coefficients of the second layer of the diffusion model have differences of less than 20% compared with those of the muscle layer of the Monte Carlo simulations if the thickness of the first layer of the diffusion model is also fitted. If l_2 is known, the differences are less than 5%, whereas the use of a semi-infinite model delivers differences of up to 55%. Even if l_2 is only approximately known the absorption coefficient of the muscle can be determined accurately. Experimentally, the time-resolved reflectance was measured on the forearms of volunteers at two distances from the incident beam by means of a streak camera. The thicknesses of the tissues involved were determined by ultrasound. The optical coefficients were derived from these measurements by applying the two-layered diffusion model, and results in accordance with the theoretical studies were observed.

1. Introduction

In recent years, considerable efforts have been devoted to determine non-invasively the optical properties of tissue, which can be applied in many fields of medicine for diagnostic purposes. The derivation of the absorption and scattering coefficients of tissue requires a theoretical model for the photon propagation in tissue. The transport theory and its approximation, the diffusion theory, have been successfully employed to calculate the photon propagation not only in tissue but also in other turbid media (Ishimaru 1978). Two extreme models are normally used to describe the geometry of the investigated tissue. The first model assumes that the optical properties of the involved tissues are homogeneous and, thus, simple solutions of the diffusion equation can be derived for the determination of the optical properties (Patterson *et al* 1989, Haskell *et al* 1994, Kienle and Patterson 1997). The second approach, in principle, does not impose any restriction on the spatial distribution of the absorption and scattering coefficients and is known as optical tomography (Yodh and Chance 1995, Arridge 1999). Due to the experimental and mathematical challenges and the ill-posed nature of the second approach (Boas *et al* 1997, Pogue *et al* 1999), the simpler homogeneous models are normally used to evaluate *in vivo* measurements.

By considering the investigated tissue as layers we apply an intermediate model that is more versatile than the homogeneous approach and more easily tractable than pure optical tomography. This is especially appealing because many tissue parts have a layered structure, for example the skin and the subcutaneous fat above the muscle in the extremities or the layers of the head above the brain. Examples for applications of the layered model are the provision of pharmacokinetic information about exogeneous chromophores in certain tissue types for photodynamic therapy (Farrell *et al* 1998, Weersink *et al* 1997) or chemotherapy (Mourant *et al* 1999), the evaluation of the depth of necroses in burns (Svaasand *et al* 1999) or the investigation of the haemodynamics in the brain to detect haemorrhages or to monitor stimulation processes (Delpy and Cope 1997, Chance *et al* 1997, Kohl *et al* 1998).

Recently, we derived solutions of the diffusion equation for a two-layered geometry having an infinitely thick second layer in the steady-state, frequency and time domains. These solutions were fitted to Monte Carlo simulations and phantom experiments (Kienle *et al* 1998a, b). In the time domain, for example, we found that it is sufficient to measure the relative time-resolved reflectance at two distances from the incident source to obtain accurate estimates of the optical coefficients of the two layers. Time-domain measurements have the advantage that the photons that have experienced a small number of scattering events and, thus, do not fulfil the diffusion approximation, can be easily disregarded. Under specific conditions where the diffusion equation is not valid, for example at small distances from the source, its application deteriorates considerably the determination of the optical coefficients (Kienle *et al* 1998a, Alexandrakis *et al* 1998, Bevilacqua and Depeursinge 1999).

In this study we investigate the usefulness of the two-layered diffusion model to determine non-invasively the haemodynamics of muscles in the extremities. We concentrate mainly on the determination of the absorption coefficient of the muscle layer, because knowledge of the absorption coefficient at several wavelengths allows one to calculate the blood oxygenation, blood flow and oxygen consumption of the muscle (Fantini *et al* 1995, Ferrari *et al* 1997). In the literature homogeneous models were used to derive the optical properties in these measurements. However, it has been recognized that the results of those models deteriorate with increasing thickness of the tissue layers above the muscle (Homma *et al* 1996, Franceschini *et al* 1998), because the probability that the photons have propagated through the muscle layer decreases. Increasing the distance between the source and detector allows us to measure photons that have penetrated deeper in the tissue. However, we have shown that increasing this distance results only in a relatively small improvement of the derived absorption coefficient of the muscle (Kienle *et al* 1998b).

In this study Monte Carlo simulations were applied to calculate the time-resolved reflectance of a three-layered model comprising skin, fat and muscle. The thickness of the fat layer above the muscle layer was altered, as was the absorption coefficient of the muscle layer to simulate haemodynamics measurements. We fitted the time-resolved reflectance of these simulated data simultaneously at two distances using the solution of the diffusion equation of a two-layered geometry. The fitting parameters were the absorption and the reduced scattering coefficients of both layers and the thickness of the first layer. In addition, we investigated the parameters obtained when the thickness of the layers above the muscle layer is known. For comparison, we also used a semi-infinite diffusion model to fit the time-resolved reflectance.

We performed time-resolved measurements on the forearms of volunteers using a streak camera. The thicknesses of the skin and subcutaneous fat layer were determined with an ultrasound apparatus. Additionally, the thickness of the tissue layers above the muscle layer was measured with a skin-fold caliper. We used the solution of the diffusion equation of a two-layered turbid medium to derive the optical coefficients from the measurements on the

forearms at two distances. As in the theoretical work, the nonlinear regressions were performed with and without fitting the thickness of the first layer of the diffusion model.

2. Theory

2.1. Diffusion equation

In this section we summarize the solutions of the diffusion equation for a semi-infinite and two-layered geometry that has been presented elsewhere (Kienle *et al* 1998a, b) and whose derivation is based on the Fourier transform technique (Dayan *et al* 1992). We give details of the numerical evaluation of the two-layered solution in the appendix. For the derivation of both equations it was assumed that a pencil beam is incident along the z -direction perpendicular to the surface of the turbid medium and that all photons are scattered at a depth $z = z_0 = 1/(\mu'_s + \mu_a)$ under the surface, where μ'_s and μ_a are the reduced scattering and the absorption coefficients of the turbid medium (first layer of the two-layered medium). Assuming a refractive index of $n_o = 1$ outside and of $n_i = 1.4$ inside the turbid medium the experimentally observed reflectance $R(\rho, t)$ from the turbid medium can be calculated with (Kienle *et al* 1998a)

$$R(\rho, t) = 0.118\Phi(\rho, z = 0, t) + 0.306D \frac{\partial}{\partial z} \Phi(\rho, z, t)|_{z=0} \quad (1)$$

where $D = 1/3(\mu_a + \mu'_s)$ is the diffusion coefficient of the turbid medium (first layer of the two-layered medium) and ρ is the radial distance between the incident beam and the surface point considered. For the semi-infinite geometry the fluence rate Φ is given by (Patterson *et al* 1989)

$$\Phi(\rho, z, t) = \frac{c}{(4\pi Dct)^{3/2}} \exp(-\mu_a ct) \times \left[\exp\left(-\frac{(z - z_0)^2 + \rho^2}{4Dct}\right) - \exp\left(-\frac{(z + z_0 + 2z_b)^2 + \rho^2}{4Dct}\right) \right] \quad (2)$$

where c is the speed of light in the turbid medium. The extrapolated boundary is located at $z = -z_b$, where

$$z_b = \frac{1 + R_{\text{eff}}}{1 - R_{\text{eff}}} 2D. \quad (3)$$

R_{eff} represents the fraction of photons that are internally diffusely reflected at the boundary. R_{eff} equals 0.493 for $n_o = 1$ and $n_i = 1.4$ (Haskell *et al* 1994). In order to obtain the time-domain reflectance for a two-layered medium having a first layer thickness l and an infinitely thick second layer, we first compute the reflectance in the frequency domain. The reduced scattering and absorption coefficient of the layer i are denoted by μ'_{si} and μ_{ai} . The fluence rate of the two-layered turbid medium is calculated with (Kienle *et al* 1998a)

$$\Phi(\rho, z, \omega) = \frac{\exp(j\omega t)}{2\pi} \int_0^\infty \phi(z, \omega, s) s J_0(s\rho) ds \quad (4)$$

where J_0 is the Bessel function of zeroth order, $j = \sqrt{-1}$ and the frequency of the sinusoidally modulated source is $f = \omega/2\pi$. The function $\phi(z, \omega, s)$ and its approximation for avoidance of numerical errors are given in the appendix. The time-domain reflectance is obtained by calculation of the real and imaginary part of the frequency domain reflectance at many frequencies and by fast Fourier transform of these data (Kienle *et al* 1998a).

2.2. Monte Carlo simulation

Monte Carlo simulations were used to calculate the time-resolved reflectance from a three-layered turbid medium (Kienle 1995). We programmed a code that uses the following variance reduction scheme to improve its efficiency. The simulations were run with zero absorption, and the absorption coefficients of the layers were considered afterwards using Beer's law (Graaff *et al* 1993). This allowed us, in addition, to calculate from one simulation the reflectance for different absorption coefficients of the third layer to simulate haemodynamics measurements in the muscle.

A pencil beam was assumed for perpendicular illumination of the turbid medium. The scattering angle was calculated using the Henyey–Greenstein phase function (Henyey and Greenstein 1941), that has an anisotropy factor of $g = 0.8$. The refractive index inside and outside the turbid medium was assumed to be 1.4 and 1.0 respectively.

2.3. Nonlinear regression

The solutions of the diffusion equation are applied to fit the Monte Carlo data in section 4 and the experimental reflectance in section 5 using a nonlinear regression routine described in the literature (Bevington 1983). Time-resolved reflectance curves at two distances were used in the nonlinear regression. In section 4.1 seven parameters, the reduced scattering and the absorption coefficients of both layers, the thickness of the first layer and two multiplicative constants accounting for the relative measurements of the reflectance at the two distances, were fitted. In section 4.2 six fitting parameters were used: the ones aforementioned without the thickness of the first layer. The time range for the nonlinear regression of $R(\rho, t)$ was chosen as follows: the start time was at $0.9R_{\max}$ (before R_{\max}) and the end time was at $R_{\max}/1000$, where R_{\max} is the maximum value of the reflectance curve. Thus, early times, where the diffusion approximation is not valid, are excluded. The time range was accordingly shortened for Monte Carlo simulations and experiments that had poor signal to noise ratio at long time values. The weights for the least-squares calculations were obtained from Poisson statistics in the case of the experimental reflectance. The statistical uncertainties used for calculation of the weights of the Monte Carlo simulations were computed from the output of several simulations having the same set of optical coefficients.

3. Materials and methods

The time-resolved reflectance on the forearm of six volunteers was measured with an apparatus that has been described in detail elsewhere (Glanzmann *et al* 1999). A dye laser that was pumped by a mode-locked and frequency-doubled Nd:YLF laser served as the light source. The pulse duration was about 10 ps and the emission wavelength was $\lambda = 830$ nm. The light was delivered via a fibre with a 600 μm core diameter. The same type of fibre was used to detect the re-emitted light. A holding device that did not disturb the mismatched boundary condition assumed in the theory ensured that the two fibres were in contact with the skin at a precise distance from each other. A streak camera with a temporal resolution of 25 ps in the used time window served as the detector. In the nonlinear regression to the experimental reflectance the theoretical data were convolved with the experimental pulse. For this purpose, the laser pulse was measured with the streak camera before each measurement on the forearm. In addition, these measurements allowed us to determine the zero time of the reflectance curves (Kienle *et al* 1998b).

The thicknesses of the tissue layers of the forearm were determined with an ultrasound apparatus (7.5 MHz). These measurements allowed us to obtain the thicknesses of the skin

and the subcutaneous fat layer (and the fascia) with an error of about 0.5 mm (including the variation of the layer thicknesses at different locations on the forearm). In addition, a skin-fold caliper, that measures mechanically the thickness of the layers above the muscle layer, was used. The main problem of this measurement device is the compression of the fat layer (Wirth 1997). The precision of this device in determining the thickness of the layers above the muscle layer is about 1 mm for medium subcutaneous fat layer thicknesses.

4. Determination of the optical properties from nonlinear regression to Monte Carlo simulations

In this section we present results obtained from nonlinear regression of the solution of the diffusion equation for a two-layered turbid medium to reflectance data calculated with three-layered Monte Carlo simulations. Besides the reduced scattering and the absorption coefficients of both layers we fitted the thickness of the first layer of the diffusion model (section 4.1), whereas in section 4.2 we assume that this quantity is known. Time-resolved reflectance at $\rho = 10.5$ and $\rho = 20.5$ mm were simultaneously fitted in both sections.

The optical coefficients used in the Monte Carlo simulations were obtained by approximately matching the measurements of the time-resolved reflectance curves on the forearms of six volunteers with theoretical reflectance by considering the optical coefficients for skin (Roggan 1997, Kienle and Hibst 1995), fat (Mitic *et al* 1994, Kienle 1995) and muscle (Pifferi *et al* 1998, Kienle 1995, Cubeddu *et al* 1999) tissue in the literature (see table 1). (Thus, it was possible to use realistic optical properties from the rather large range of values found in the literature.) Figure 1 shows $R(\rho, t)$ measured on the forearms of six volunteers at $\rho = 11.8$ mm. The thickness of the skin and subcutaneous fat layer was determined with ultrasound measurements (see figure 1). It can be seen that the shape of the time-resolved reflectance curves is broadened with increasing thickness of the subcutaneous fat layer, mainly due to the low absorption of the fat. In the Monte Carlo simulations the thickness of the skin was assumed to be 1.2 mm, whereas that of the muscle was taken as infinite. The thickness of the subcutaneous fat layer was varied, so that the skin and the subcutaneous fat layers equalled together $l_2 = 2, 5$ and 10 mm (see table 1). (l_2 denotes the thickness of the skin and subcutaneous fat layer in the Monte Carlo simulations or experiments, whereas l describes the thickness of the first layer in the diffusion model. Parameters obtained by nonlinear regression are indicated by an asterisk.) The absorption coefficient of the muscle layer was varied to account for the variation of the blood content in the muscle and to simulate haemodynamics measurements.

Table 1. Optical coefficients and layer thicknesses used in the Monte Carlo simulations.

Tissue	Thickness (mm)	μ'_s (mm ⁻¹)	μ_a (mm ⁻¹)
Skin	1.2	1.5	0.015
Fat	0.8/3.8/8.8	1.2	0.002
Muscle	∞	0.5	0.02–0.03

4.1. Nonlinear regression including the first layer thickness as fitting parameter

In figures 2, 3 and 4 the estimated absorption coefficients, reduced scattering coefficients and thicknesses of the first layer of the diffusion model obtained from the regressions are compared with the parameters used in the Monte Carlo simulations. The results for $l_2 = 5$ mm (circles)

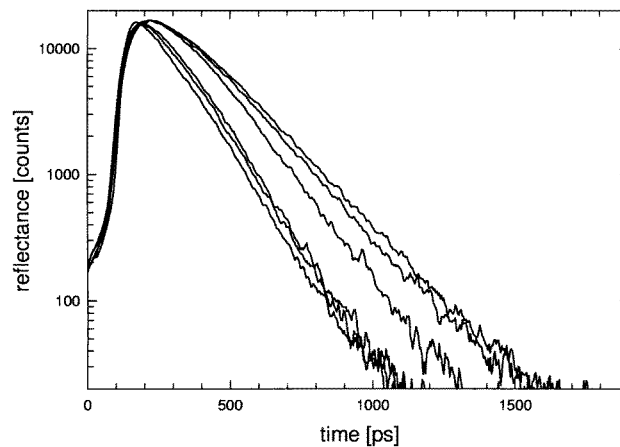


Figure 1. Time-resolved reflectance measurements on the forearm of six volunteers. The thicknesses of the tissue layers above the muscle layer were determined from ultrasound measurements as 2.0, 2.7, 2.7, 3.4, 5.0 and 5.0 mm (beginning with the narrowest to the broadest curve).

and $l_2 = 10$ mm (squares) can be seen in the figures, whereas those for $l_2 = 2$ mm are not shown, because in the latter case the χ^2 -space has a shallow shape around the minimum, so that the nonlinear regression converges very slowly and, thus, considerably different parameters deliver almost the same goodness of fit. (However, μ_{a2}^* had differences of only a few per cent compared with the absorption coefficient of the third layer in the Monte Carlo simulations.) The figures show that for $l_2 = 5$ mm the estimated optical coefficients of the second layer of the diffusion model are close to the optical coefficients of the third layer of the Monte Carlo simulations. In particular the differences in determining μ_{a3} are only about 2%. The estimated absorption coefficients of the first layer (μ_{a1}^*) are close to the absorption coefficients of the second layer of the Monte Carlo simulations (μ_{a2}), whereas the estimated reduced scattering coefficients of the first layer (μ_{s1}^*) are between those of the first and second layer of the Monte Carlo simulations. The estimated thicknesses of the first layer l^* are about 10% less than the thickness of the first two layers of the Monte Carlo simulations. We note that we also performed Monte Carlo simulations for $l_2 = 5$ mm and other optical properties that were reported in the literature for skin, fat and muscle. In general, although the features of the estimated parameters showed considerable differences from the above ones (for example the estimated thickness of the first layer was $l^* \approx 3$ mm for some cases), the estimated absorption coefficients of the second layer (μ_{a2}^*) showed differences $\lesssim 10\%$ compared with μ_{a3} .

For $l_2 = 10$ mm the estimated absorption and reduced scattering coefficients of the second layer of the diffusion model show greater differences than those of the third layer of the Monte Carlo simulations compared with $l = 5$ mm. This is probably caused by the smaller probability that a detected photon has experienced the muscle layer for $l_2 = 10$ mm compared with $l_2 = 5$ mm, so that the reflectance curves are less influenced by the muscle layer. However, the differences between μ_{a2}^* and μ_{a3} are less than 20%.

4.2. Nonlinear regression knowing the layer thicknesses

In order to accelerate the convergence of the nonlinear regressions and to improve the determination of the absorption coefficients of the muscle, we performed nonlinear regressions

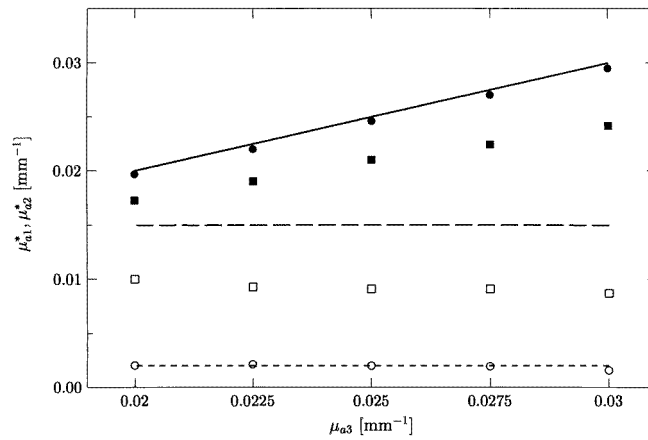


Figure 2. Estimated absorption coefficients of both layers (μ_{a1}^* (open symbols), μ_{a2}^* (full symbols)) determined by nonlinear regressions of time-resolved reflectance using the two-layered solution of the diffusion equation to three-layered Monte Carlo data are shown versus the absorption coefficient of the third layer used in the Monte Carlo simulations (μ_{a3}). The thicknesses of the first two layers are $l_2 = 5$ mm (circles) and $l_2 = 10$ mm (squares). The lines indicate μ_{a1} (long dashed), μ_{a2} (short dashed) and μ_{a3} (full).

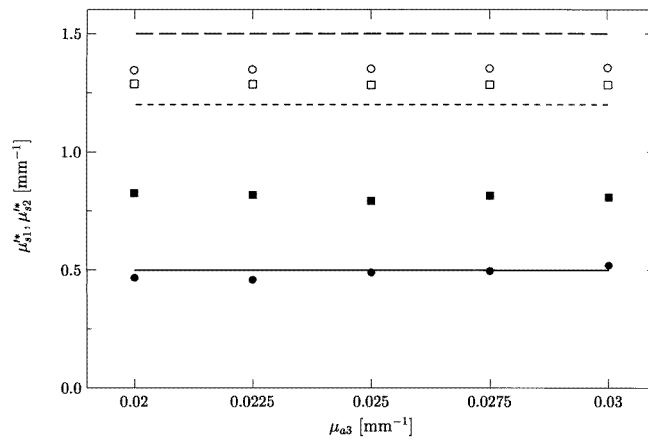


Figure 3. Estimated reduced scattering coefficients of both layers (μ_{s1}^* (open symbols), μ_{s2}^* (full symbols)) determined by nonlinear regressions of time-resolved reflectance using the two-layered solution of the diffusion equation to three-layered Monte Carlo data are shown versus the absorption coefficient of the third layer used in the Monte Carlo simulations (μ_{a3}). The thickness of the first two layers are $l_2 = 5$ mm (circles) and $l_2 = 10$ mm (squares). The lines indicate μ_{s1}^* (long dashed), μ_{s2}^* (short dashed) and μ_{s3}^* (full).

assuming that l_2 is known and is equal to the first layer thickness of the diffusion model. Figure 5 shows the estimated absorption coefficient of the second layer (μ_{a2}^*) for $l_2 = 2$ mm (open circles), 5 mm (crosses) and 10 mm (full circles). The absorption coefficients (μ_{a3}) of the muscle tissue can be obtained with differences less than 2% for $l_2 = 2$ and 5 mm, whereas μ_{a2}^* is systematically smaller than μ_{a3} for $l_2 = 10$ mm. However, the differences are less than 5%. For comparison, figure 5 also shows the absorption coefficients (μ_a^*) obtained from

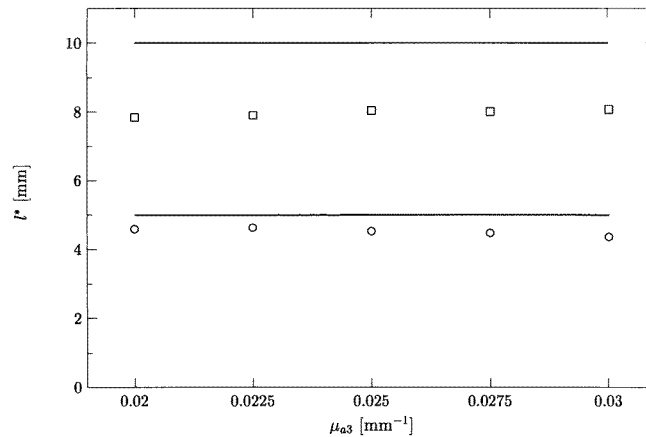


Figure 4. Estimated thickness of the first layer l^* determined by nonlinear regressions of time-resolved reflectance using the two-layered solution of the diffusion equation to three-layered Monte Carlo data are shown versus the absorption coefficient of the third layer used in the Monte Carlo simulations (μ_{a3}). The thicknesses of the first two layers are $l_2 = 5$ mm (circles) and $l_2 = 10$ mm (squares) as indicated by lines.

nonlinear regressions of the solution of the semi-infinite medium to the three-layered Monte Carlo simulations for $l_2 = 2$ mm (open squares), 5 mm (plusses) and 10 mm (triangles). Time-resolved reflectance data at 20.5 mm were used. The differences between μ_a^* and the absorption coefficient of the muscle used in the Monte Carlo simulations are less than 2% for $l_2 = 2$ mm, up to 13% for $l_2 = 5$ mm and up to 55% for $l_2 = 10$ mm. (These results are in accordance with those of Franceschini *et al* (1998) who found that the measured effective optical coefficients of a two-layered tissue are 'representative of the underlying block if the superficial layer is less than ≈ 0.4 cm'.) The differences increase for increasing l_2 as well as for increasing μ_{a3} , because the probability that a photon has propagated through the muscle layer and is detected is decreased. The corresponding reduced scattering coefficients estimated from the nonlinear regressions using both the solution of the diffusion equation for a two-layered medium as well as for a semi-infinite medium are shown in figure 6. Similar to the determination of the absorption coefficients, the differences between the estimated reduced scattering coefficients of the second layer of the diffusion model and those of the muscle layer used in the Monte Carlo simulations are smaller for smaller l_2 and in the case of the two-layered model compared with the semi-infinite model. In general, the estimated reduced scattering coefficients show larger differences than the absorption coefficients.

We have assumed in the calculations so far in this section that the thickness of the layers above the muscle layer is exactly known. We also investigated the influence on the estimated optical coefficients when the assumed value of the layers above the muscle layer in the diffusion model deviates from its true value. Figure 7 shows the estimated absorption coefficients of the second layer for $l_2 = 2$ mm (crosses), 5 mm (full circles) and 10 mm (open circles) versus l for $\mu_{a3} = 0.025$ mm $^{-1}$. In general, μ_{a2}^* is only weakly dependent on the assumed l . The estimated μ_{a2}^* have differences of less than 2%, 6% and 17% compared with the absorption coefficient of the muscle layer for $l_2 = 2, 5$ and 10 mm respectively. Contrarily, μ_{a1}^* and μ_{s2}^* show a large dependence on l (data not shown). For large differences between l and l_2 the fit diverges, because either μ_{a1}^* or μ_{s2}^* becomes negative.

Figure 8 shows the estimated absorption coefficients of the second layer of the diffusion model versus μ_{a3} for $l_2 = 5$ mm assuming in the nonlinear regression that $l = 4$ mm

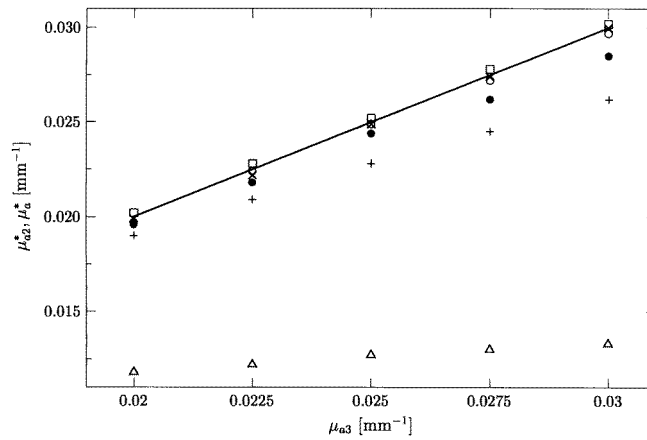


Figure 5. Estimated absorption coefficients of the second layer (μ_{a2}^*) determined by nonlinear regressions of time-resolved reflectance using the two-layered solution of the diffusion equation to three-layered Monte Carlo data are shown versus the absorption coefficient of the third layer used in the Monte Carlo simulations (μ_{a3}). In the nonlinear regression it is assumed that l_2 is known. Results are presented for $l_2 = 2$ mm (open circles), $l_2 = 5$ mm (crosses) and $l_2 = 10$ mm (full circles). The line indicates μ_{a3} . Additionally, estimated absorption coefficients (μ_{a2}^*) obtained from a semi-infinite model for $l_2 = 2$ mm (open squares), $l_2 = 5$ mm (plusses) and $l_2 = 10$ mm (triangles) are shown.

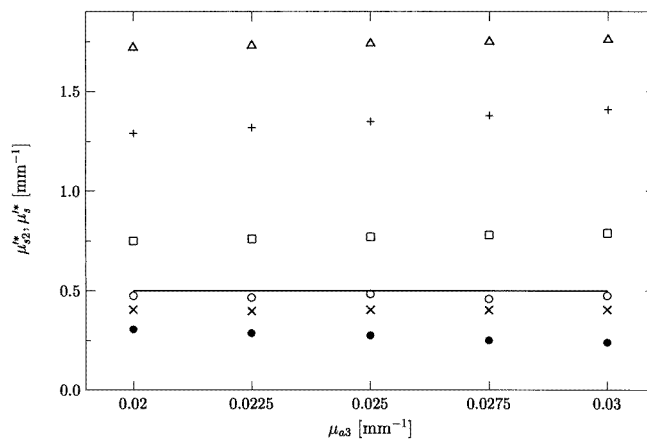


Figure 6. Estimated reduced scattering coefficients of the second layer (μ_{s2}^*) determined by nonlinear regressions of time-resolved reflectance using the two-layered solution of the diffusion equation to Monte Carlo data are shown versus the absorption coefficient of the third layer used in the three-layered Monte Carlo simulations (μ_{a3}). In the nonlinear regression it is assumed that l_2 is known. Results are presented for $l_2 = 2$ mm (open circles), $l_2 = 5$ mm (crosses) and $l_2 = 10$ mm (full circles). The line indicates μ_{s3} . Additionally, estimated reduced scattering coefficients (μ_{s2}^*) obtained from a semi-infinite model for $l_2 = 2$ mm (open squares), $l_2 = 5$ mm (plusses) and $l_2 = 10$ mm (triangles) are shown.

(full circles), $l = 6$ mm (crosses) and $l = 7$ mm (open circles). The estimated μ_{a2}^* have differences less than 4% compared with the absorption coefficients of the muscle layer for all l_2 . In addition, the differences are similar for a certain l_2 and different μ_{a3} . For example, μ_{a2}^* is

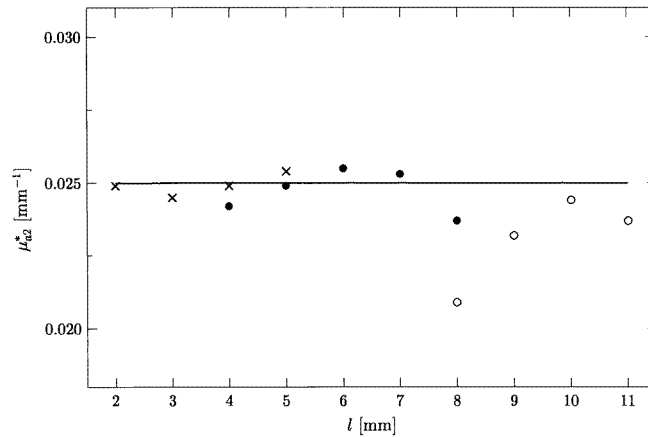


Figure 7. Estimated absorption coefficients of the second layer (μ_{a2}^*) determined by nonlinear regressions of time-resolved reflectance using the two-layered solution of the diffusion equation to three-layered Monte Carlo data are shown versus the assumed thickness of the layers above the muscle layer (l). Estimated μ_{a2}^* obtained for $l_2 = 2$ mm (crosses), $l_2 = 5$ mm (full circles) and $l_2 = 10$ mm (open circles) are shown. The line indicates $\mu_{a3} = 0.025$ mm $^{-1}$.

Table 2. Estimated parameters and uncertainties determined by nonlinear regression of the two-layered solution of the diffusion equation to measurements on the forearm.

l_2 (mm)	μ_{s1}^* (mm $^{-1}$)	μ_{a1}^* (mm $^{-1}$)	μ_{s2}^* (mm $^{-1}$)	μ_{a2}^* (mm $^{-1}$)
$5.3' \pm 0.5$	$1.55' \pm 0.02$	$0.0023' \pm 0.0004$	$0.39' \pm 0.03$	$0.0238' \pm 0.0006$
5	1.57 ± 0.03	0.0016 ± 0.0015	0.44 ± 0.02	0.0239 ± 0.0013
6	1.50 ± 0.02	0.0033 ± 0.0010	0.28 ± 0.02	0.0236 ± 0.0013
7	1.44 ± 0.02	0.0037 ± 0.0007	0.13 ± 0.02	0.0226 ± 0.0016

always about 0.008 mm $^{-1}$ smaller than μ_{a3} for $l = 4$ mm. This is important when changes in the absorption coefficient are monitored such as for oxygenation measurements under different physiological conditions.

5. Determination of the optical properties from nonlinear regression to *in vivo* experiments

Measurements of the time-resolved reflectance on a human forearm at $\rho = 16.3$ mm and $\rho = 20.3$ mm can be seen in figure 9. The thickness of the layers above the muscle layer was determined to be $l_2 = 5$ mm by ultrasound. Also shown are the results of the nonlinear regression of the solution of the diffusion equation for a two-layered medium assuming that the thickness of the involved layers is not known. Table 2 gives the optical parameters obtained from nonlinear regression by fitting the optical coefficients and l (indicated by ') and from nonlinear regression by assuming that the thickness of the layers above the fat layer is known. The true value ($l = 5$ mm) as well as false values ($l = 6$ and 7 mm) were assumed. For other values of l the fit diverged. Similar to the nonlinear regression for the three-layered Monte Carlo simulations, the absorption coefficient of the second layer of the diffusion model is relatively independent of the choice of l , whereas μ_{a1}^* and μ_{s2}^* show a strong dependence on l . The semi-infinite solution was also fitted to the time-resolved reflectance measurements.

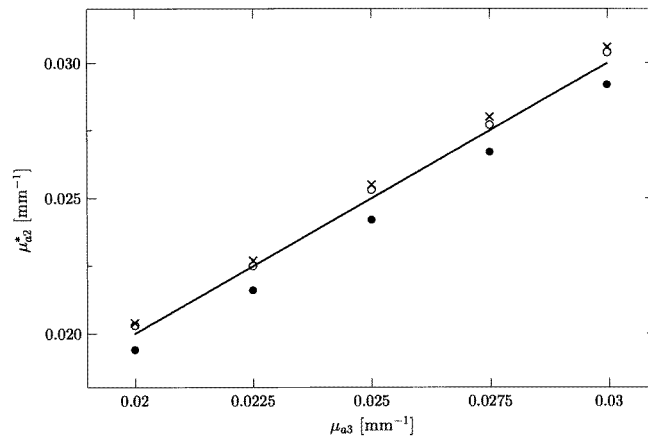


Figure 8. Estimated absorption coefficients of the second layer (μ_{a2}^*) determined by nonlinear regressions of time-resolved reflectance using the two-layered solution of the diffusion equation to three-layered Monte Carlo data are shown versus the absorption coefficient of the third layer used in the Monte Carlo simulations (μ_{a3}). The layers above the muscle layer have a thickness of $l_2 = 5$ mm in these simulations. In the nonlinear regression it is assumed that $l = 4$ mm (full circles), $l = 6$ mm (crosses) and $l = 7$ mm (open circles).

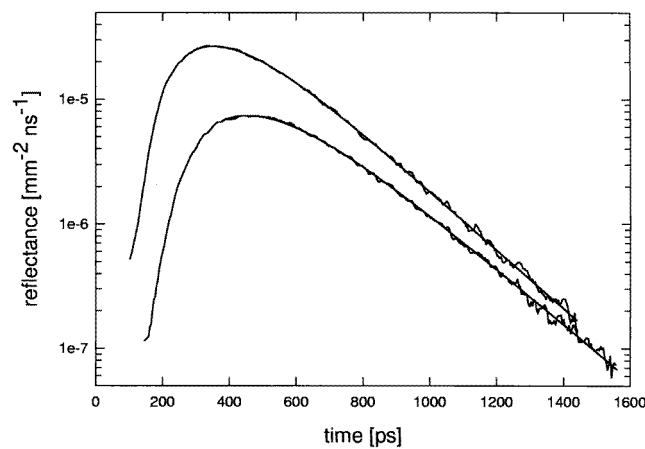


Figure 9. Experimental time-resolved reflectance on a human forearm at $\rho = 16.3$ mm and $\rho = 20.3$ mm (noisy curves) and results of the nonlinear regression.

For $\rho = 20.3$ mm we obtained $\mu_s^{*s} = 1.07 \text{ mm}^{-1}$ and $\mu_a^* = 0.019 \text{ mm}^{-1}$. Similar to the theoretical work, μ_a^* obtained with the semi-infinite model is smaller than that calculated with the two-layered model (see figure 5).

The nonlinear regressions to the measurements on the forearms of the other volunteers gave, in general, similar results. However, for several measurements it was not possible to obtain a reasonable fit (see below).

6. Discussion

In this study we investigated the use of a solution of the diffusion equation for two layers to obtain the optical properties of muscle tissue in the extremities. By fitting this solution to three-layered Monte Carlo simulations (representing skin, fat and muscle) we found that the absorption coefficient of the second layer in the diffusion model is, in general, close to the absorption coefficient of the muscle layer in the Monte Carlo simulation. This was found for nonlinear regression including and excluding the thickness of the first layer in the diffusion model as fitting parameter. However, including this parameter in the fit causes the nonlinear regression to converge very slowly, indicating a very smooth χ^2 surface. Therefore, a systematic error in the measurements can greatly influence the optical properties obtained.

The nonlinear regressions are more stable if the thickness of the layers above the muscle layer is known and is used as thickness of the first layer of the two-layered diffusion model. We showed that the estimated μ_{a2}^* has differences of only a few per cent compared with the absorption coefficient of the muscle layer in the Monte Carlo simulations in this case. Additionally, we found that the absorption coefficient of the muscle can still be accurately determined even if l_2 is not exactly known. For large thicknesses of the layers above the muscle layer ($l_2 = 10$ mm) we found systematic differences between μ_{a2}^* and μ_{a3} (see figure 5). However, these differences are less than 5%. In contrast, the use of the semi-infinite diffusion solution results in differences of up to 55% for this l_2 .

Measurements on the human forearms of volunteers were performed at different distances. We showed for measurements on a forearm with a thickness of the skin and subcutaneous fat layer of 5 mm that the estimated optical coefficients using the two-layered diffusion equation solutions are in accordance with the theoretical investigations. We found, for example, that the estimated μ_{a2}^* changed only by 1% and 5% assuming $l = 6$ mm and $l = 7$ mm compared with the true value ($l = 5$ mm) respectively. (For other values of l the nonlinear regression diverged.) Therefore, it is not necessary to know exactly the thickness of the layers above the muscle layer to obtain good estimates of the absorption coefficient of the muscle layer. (Skin-fold caliper measurements or even manual estimates might be sufficient.) The estimated reduced scattering coefficient of the muscle, however, is largely influenced by the choice of l (see the theoretical data in figure 6 and the experimental data in table 2). In general, the derived reduced scattering coefficients of the second layer in the diffusion model show larger differences than those of the muscle layer compared with the absorption coefficients, but the differences are much smaller than those obtained from the semi-infinite model.

A disadvantage of the two-layered solution, besides its more complicated and slower mathematical evaluation, is that the nonlinear regression is less robust to systematical errors in the measurements compared with the semi-infinite model. For the measurements of the time-resolved reflectance the zero time was obtained by an additional measurement of the laser pulse before each measurement on the forearm. Thus, the determination of the zero time depended on the stability of the laser source. To investigate the influence of this quantity we fitted the two-layered diffusion equation to Monte Carlo data where the zero time was changed. It was found that a shift of the zero time of about 40 ps can cause considerably different optical properties. Thus, it is not surprising that the nonlinear regressions to some forearm measurements gave poor fits, because the jitter of our system was in the range of 40 ps during the time between the measurement of the zero time and the forearm measurements. Therefore, we recommend measuring the incident laser beam simultaneously with the *in vivo* measurement to avoid this problem.

In summary, we showed that for thicknesses of the skin and the subcutaneous fat layer of up to $l_2 = 10$ mm the absorption coefficient of the muscle in the extremities can be derived accurately using a solution of the diffusion equation for two layers, if l_2 is approximately known.

The relatively small distances used for the measurements of the time-resolved reflectance ($\rho < 21$ mm) enable a relatively high spatial resolution for imaging purposes. It has to be investigated if a two-layered model can also be used for other applications, such as the determination of the absorption coefficient of the brain, or if this model has to be extended to more layers. This would, probably, imply either an *a priori* knowledge of the optical coefficients of some layers or measurements of the time-resolved reflectance at more than two distances (Tualle *et al* 1996).

Acknowledgments

The authors are indebted to Dr G Wagnires and Professor H van den Bergh for the opportunity to perform the time-resolved measurements. We would like to thank Dr H Wenzel for the provision of the skin-fold caliper, and Dr P Grosjean and Dr M Reber for performing the ultrasound measurements.

Appendix

The function $\phi(z, \omega, s)$ introduced in section 2 is given by

$$\phi(z, \omega, s) = \frac{\sinh[\alpha_1(z_b + z_0)]}{D_1\alpha_1} \left\{ \frac{D_1\alpha_1 \cosh[\alpha_1(l - z)] + D_2\alpha_2 \sinh[\alpha_1(l - z)]}{D_1\alpha_1 \cosh[\alpha_1(l + z_b)] + D_2\alpha_2 \sinh[\alpha_1(l + z_b)]} \right\} - \frac{\sinh[\alpha_1(z_0 - z)]}{D_1\alpha_1} \quad 0 \leq z < z_0 \quad (5)$$

where we assumed that $l > z_0$. $D_i = 1/(3(\mu_{ai} + \mu'_{si}))$ is the diffusion coefficient of layer i and $\alpha_i^2 = (D_i s^2 + \mu_{ai} + j\omega/c)/D_i$. In order to avoid numerical errors in the calculation of equation (5) limiting equations are derived. Expressing the hyperbolic functions with exponentials it follows for the term in curly brackets in equation (5) ($z = 0$)

$$\frac{\exp(\alpha_1 l)(D_1\alpha_1 + D_2\alpha_2) + \exp(-\alpha_1 l)(D_1\alpha_1 - D_2\alpha_2)}{\exp[\alpha_1(l + z_b)](D_1\alpha_1 + D_2\alpha_2) + \exp[-\alpha_1(l + z_b)](D_1\alpha_1 - D_2\alpha_2)} = \frac{1 + D_a \exp(-2\alpha_1 l)}{\exp(\alpha_1 z_b)\{1 + D_a \exp[-2\alpha_1(l + z_b)]\}} \quad (6)$$

where $D_a = (D_1\alpha_1 - D_2\alpha_2)/(D_1\alpha_1 + D_2\alpha_2)$. For $\phi(z = 0, \omega, s)$ we get

$$\phi(z = 0, \omega, s) = (\{\exp(\alpha_1 z_0) - \exp[-\alpha_1(2z_b + z_0)]\} \frac{1 + D_a \exp(-2\alpha_1 l)}{1 + D_a \exp[-2\alpha_1(l + z_b)]} - [\exp(\alpha_1 z_0) - \exp(-\alpha_1 z_0)]/2D_1\alpha_1) \quad (7)$$

For $2\alpha_1(l + z_b) \gg 1$ the denominator in equation (7) can be expanded, and, thus, $\phi(z = 0, \omega, s)$ can be expressed as a sum of exponential terms. For example, to first order in D_a we get

$$\phi(z = 0, \omega, s) \approx (\exp(-\alpha_1 z_0) - \exp[-\alpha_1(2z_b + z_0)] + D_a \{\exp[\alpha_1(z_0 - 2l)] - \exp[\alpha_1(-z_0 - 2l - 2z_b)] - \exp[\alpha_1(z_0 - 2l - 2z_b)] + \exp[\alpha_1(-z_0 - 2l - 4z_b)]\})/2D_1\alpha_1) \quad (8)$$

References

- Alexandrakis G, Farrell T J and Patterson M S 1998 Accuracy of the diffusion approximation in determining the optical properties of a two-layer turbid medium *Appl. Opt.* **37** 7401–10
 Arridge S R 1999 Optical tomography in medical imaging *Inverse Problems* **15** R41–R93
 Bevilacqua F and Depierreux C 1999 Monte Carlo study of diffuse reflectance at source-detector separations close to one transport mean free path *J. Opt. Soc. Am. A* accepted

- Bevington P R 1983 *Data Reduction and Error Analysis for the Physical Sciences* (New York: McGraw-Hill)
- Boas D A, O'Leary M A, Change B and Yodh A G 1997 Detection and characterization of optical inhomogeneities with diffuse photon density waves: a signal-to-noise analysis *Appl. Opt.* **36** 75–92
- Chance B, Luo Q, Nioka S, Alsop D C and Detre J A 1997 Optical investigations of physiology: a study of intrinsic and extrinsic contrast *Phil. Trans. R. Soc. B* **352** 707–16
- Cubeddu R, Pifferi A, Taroni P, Torricelli A and Valentini G 1999 Compact tissue oximeter based on dual-wavelength multichannel time-resolved reflectance *Appl. Opt.* **38** 3670–80
- Dayan I, Havlin S and Weiss G H 1992 Photon migration in a two-layer turbid medium. A diffusion analysis *J. Mod. Opt.* **39** 1567–82
- Delpy D T and Cope M 1997 Quantification in tissue near-infrared spectroscopy *Phil. Trans. R. Soc. B* **352** 649–59
- Fantini S, Franceschini-Fantini M A, Maier J S, Walker S A, Barbieri B and Gratton E 1995 Frequency-domain multichannel optical detector for noninvasive tissue spectroscopy and oximetry *Opt. Eng.* **34** 32–42
- Farrell T J, Patterson M S and Essenpreis M 1998 Influence of layered tissue architecture on estimates of tissue optical properties obtained from spatially resolved diffuse reflectometry *Appl. Opt.* **37** 1958–72
- Ferrari M, Binzoni T and Quaresima V 1997 Oxidative metabolism in muscle *Phil. Trans. R. Soc. B* **352** 677–83
- Franceschini M A, Fantini S, Paulescu L A, Maier J S and Gratton E 1998 Influence of a superficial layer in the quantitative spectroscopy study of strongly scattering media *Appl. Opt.* **37** 7447–58
- Glanzmann T, Ballini J-P, van den Bergh H and Wagnières G 1999 Time-resolved spectrafuorometer for clinical tissue characterization during endoscopy *Rev. Sci. Instrum.* **70** 4067–77
- Graaff R, Koelink M H, de Mul F F M, Zijlstr W G, Dassel A C M and Aarnoudse J G 1993 Condensed Monte Carlo simulations for the description of light transport *Appl. Opt.* **32** 426–34
- Haskell R C, Svaasand L O, Tsay T T, Feng T C, McAdams M and Tromberg B T 1994 Boundary conditions for the diffusion equation in radiative transfer *J. Opt. Soc. Am. A* **11** 2727–41
- Heney L G and Greenstein J L 1941 Diffuse radiation in galaxy *Astrophys. J.* **93** 70–83
- Homma S, Fukunaga T and Kagaya A 1996 Influence of adipose tissue thickness on near infrared spectroscopic signals in the measurement of human muscle *J. Biomed. Opt.* **1** 418–24
- Ishimaru A 1978 *Wave Propagation and Scattering in Random Media* (New York: Academic) chs 7, 9
- Kienle A 1995 Lichtausbreitung in biologischem Gewebe *Dissertation* University of Ulm
- Kienle A, Glanzmann T, Wagnières G and van den Bergh H 1998b Investigation of two-layered turbid media with time-resolved reflectance *Appl. Opt.* **37** 6852–62
- Kienle A and Hibst R 1995 New optimal wavelength for treatment of portwine stains? *Phys. Med. Biol.* **40** 1559–76
- Kienle A and Patterson M S 1997 Improved solutions of the steady-state and time-resolved diffusion equations for reflectance from a semi-infinite turbid medium *J. Opt. Soc. Am. A* **14** 246–54
- Kienle A, Patterson M S, Utke N, Bays R, Wagnières G and van den Bergh H 1998a Noninvasive determination of the optical properties of two-layered turbid media *Appl. Opt.* **37** 779–91
- Kohl M, Lindauer U, Dirmagl U and Villringer A 1998 Separation of changes in light scattering and chromophore concentrations during cortical spreading depression in rats *Opt. Lett.* **23** 555–7
- Mitic G, Kölzer J, Otto J, Plies E, Sölkner G and Zinsh W 1994 Time-gated transillumination of biological tissues and tissuelike phantom *Appl. Opt.* **33** 6699–710
- Mourant J R, Johnson T M, Los G and Bigio I J 1999 Non-invasive measurement of chemotherapy drug concentration in tissue: preliminary demonstrations of *in vivo* measurements *Phys. Med. Biol.* **44** 1397–417
- Patterson M S, Chance B and Wilson B C 1989 Time resolved reflectance and transmittance for the noninvasive measurement of tissue optical properties *Appl. Opt.* **28** 2331–6
- Pifferi A, Cubeddu R, Taroni P, Torelli A and Torricelli A 1998 *In vivo* absorption and scattering spectra of human tissues by time-resolved reflectance *Proc. SPIE* **3566** 230–5
- Pogue B W, McBride T O, Osterberg U L and Paulsen K D 1999 Comparison of imaging geometries for diffuse optical tomography of tissue *Opt. Express* **4** 270–86
- Roggan A 1997 Dosimetrie thermischer Laseranwendungen in der Medizin *Dissertation* Freie Universität Berlin
- Svaasand L O, Spott T, Fishkin J B, Pham T, Tromberg B J and Berns M W 1999 Reflectance measurements of layered media with diffuse photon-density waves: a potential tool for evaluating deep burns and subcutaneous lesions *Phys. Med. Biol.* **44** 801–13
- Tualle J M, Gélébart B, Tinet E, Avriillier S and Ollivier J P 1996 Real time optical coefficients evaluation from time and space resolved reflectance measurements *Opt. Commun.* **124** 216–21
- Weersink R A, Hayward J E, Diamond K R and Patterson M S 1997 Accuracy of noninvasive *in vivo* measurements of photosensitizer uptake based on a diffusion model of reflectance spectroscopy *Photochem. Photobiol.* **66** 326–35
- Wirth A 1997 *Adipositas* (Berlin: Springer)
- Yodh A and Chance B 1995 Spectroscopy and imaging with diffusing light *Phys. Today* **48** 34–40